2014 RISP International Workshop on Nonlinear Circuits,
Communications and Signal Processing
NCSP'14, Honolulu, Hawaii, USA. February 28 - March 3, 2014

Coupled Chaotic System Based on Shinriki-Mori Circuit

Tatsuki Sobue[1], Yasuteru Hosokawa[1] and Yoshifumi Nishio[2]

[1] Shikoku University
Furukawa, Ohjin, Tokushima, Japan
Phone:+81-88-665-1300
FAX:+81-88-637-1318
E-mail: s002337018@edu.shikoku-u.ac.jp
E-mail: hosokawa@keiei.shikoku-u.ac.jp

[2] Tokushima University
2-1 Minami-Josanjima, Tokushima, Japan
Phone:+81-88-656-7470
FAX:+81-88-656-7471
E-mail: nishio@ee.tokushima-u.ac.jp

Abstract

Shinriki-Mori circuit have been applied to coupled systems for investigations of a coupled system. In this study, we propose a novel coupled system based on Shinriki-Mori circuit.

1. Introduction

There are many studies about synchronization phenomena of coupled chaotic circuits. In these system, some famous chaotic circuits are applied. One of famous chaotic circuit is Shinriki-Mori circuit [1] [2]. There are many investigations about coupled chaotic circuits using this circuit. One of important factors is a parameter mismatch in these investigations. By including a parameter mismatches, some interesting phenomena are observed. In the first place, the circuit includes parameter mismatches. There are not perfectly same two things in the natural world.

However, it is not easy to change a circuit characteristic intentionally by changing parameter mismatches. Especially, switching phenomena which are very interesting phenomena are influenced by a parameter mismatches.

In this study, a novel coupled system for investigation of coupled chaotic system is proposed. This system can generate similar two chaotic waveforms intentionally. This system is also a coupled chaotic system. By investigating this system, the contribution of the field of coupled chaotic circuits is expected.

2. Circuit Model

Figure 1 shows a proposed circuit. This system is based on Shinriki-Mori circuit proposed in [1]. The modified points are follows. Right parts of the circuit are duplexed. Resistors R_n $(n = 1, 2, \cdots N)$ are added for changing a parameter of bidirectionally coupled diodes. In this study, bidirectionally coupled diodes and resistors are modeled as a piecewise linear function shown in Fig. 2.

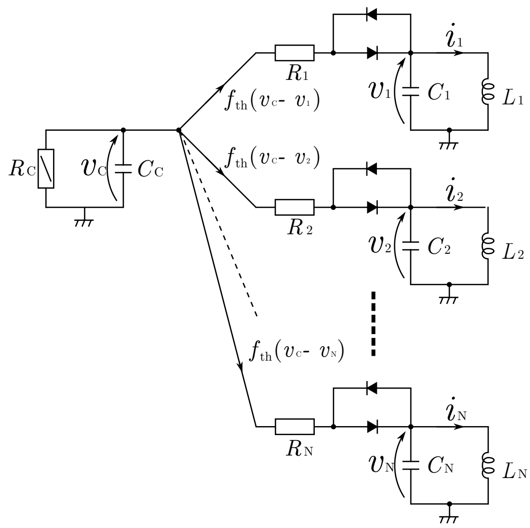

Figure 1: Proposed System.

Using this model, the circuit equation is described as follows.

$$\begin{cases} C_n \dfrac{dv_n}{dt} = \dfrac{v_c}{R_n} - f_{th}(v_c - v_n) - i_n, \\ C_c \dfrac{dv_c}{dt} = \dfrac{v_c}{R_c} - \displaystyle\sum_{n=1}^{N} \{\alpha_n f_{th}(v_c - v_n)\}, \\ L_n \dfrac{di_n}{dt} = v_n, \end{cases} \quad (1)$$

where

$$f(v) = v + (|v - V_{th}| - |v + V_{th}|)/2. \quad (2)$$

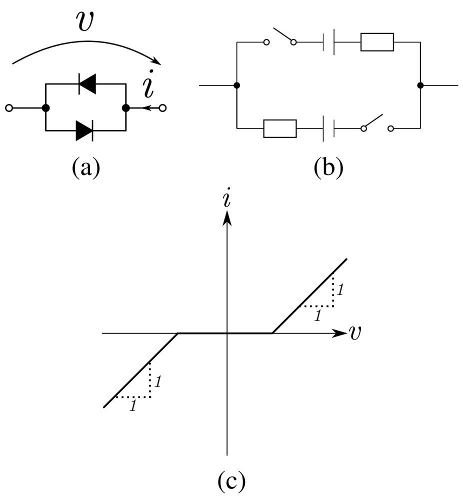

Figure 2: Bidirectionally coupled diodes model. (a) Circuit schematic. (b) Circuit model. (c) $v - i$ characteristic.

By substituting the variables and the parameters,

$$\begin{aligned}
&x_n = \frac{v_n}{V_{th}}, \quad x_{N+n} = \sqrt{\frac{L_1}{C_1}}\frac{i_n}{V_{th}}, \\
&\frac{d}{dt} = \text{“}\cdot\text{”}, \quad \tau = \frac{1}{\sqrt{L_1C_1}}t, \quad \alpha_n = \frac{1}{R_n}\sqrt{\frac{L_1}{C_1}}, \\
&\alpha_c = \frac{1}{R_c}\sqrt{\frac{L_1}{C_1}}, \quad \beta_n = \frac{C_1}{C_n}, \quad \beta_c = \frac{C_1}{C_c} \\
&\text{and} \quad \gamma_n = \frac{L_1}{L_n}, \quad (n = 1, 2, \cdots N.)
\end{aligned} \tag{3}$$

equations (1) and (2) are normalized as

$$\begin{cases}
\dot{x}_n &= \beta_n \left\{\alpha_n f(x_c - x_n) - x_{N+n}\right\}, \\
\dot{x}_{N+n} &= \gamma_n x_n, \\
\dot{x}_c &= \beta_c \left[\alpha_c x_c - \sum_{n=1}^{N} \left\{\alpha_n f(x_c - x_n)\right\}\right],
\end{cases} \tag{4}$$

where

$$f(x) = x + (|x - 1| - |x + 1|)/2. \tag{5}$$

3. Experimental Results and Computer Simulation Results

At first, the case of $N = 2$ is investigated. Figure 3 shows circuit experimental results (a) and computer simulation results (b)-(c). Parameters are set as $R_1 = R_2 = 120$ [Ω], $C_1 = C_2 = 0.015$[μF], $L_1 = L_2 = 50$[mH] in circuit experiments. $\alpha_1 = \alpha_2 = 9$, $\beta_1 = \beta_2 = 1$, $\beta_c = 0.32$ and $\gamma_1 = \gamma_2 = 1$. Control parameters are selected as R_c. Figure 3 (a) show projections of attractors onto $v_3 - x_1$ plane. Figures 3 (b) and (c) show projections of attractors onto $v_3 - x_1$ plane and $v_3 - x_1$ plane, respectively.

By changing parameter R_c and α_c, one periodic orbit (1), two periodic orbit (2), chaos (3) (4), double scroll type attractor (5), window (6) and chaos (7) are observed. In this investigation, parameters of right side elements are same. Therefore, v_1 and v_2 are synchronized as shown in Fig. 3 (c).

Figure 4-5 shows the case of applying different resistances of the right side of the system. When differences are small as shown in Fig. 4, these are synchronized. However, by increasing the differences, these become asynchronization states as shown in Fig. 5. We consider that there are possibility of applying this state to some applications because these have similar waveforms in spite of the asynchronization state.

On the other hand, the case applying same resistance and different capacitances of the right side of the system is shown in Fig. 6-7. In these cases, these are not synchronized at all. However, in the case of Fig. 6, waveforms and attractors are very similar forms.

4. Conclusion

In this study, we propose a novel coupled system based on Shinriki-Mori circuit. The relationships between observed synchronization phenomena and parameters are investigated.

In the future works, the large number N case will be investigated.

References

[1] M. Shinriki, M. Yamamoto and S. Mori, “Multimode Oscillations in a Modified van der Pol Oscillator containing a positive nonlinear conductance,” Proc. IEEE, vol. 69, no. 3, pp. 394-395, 1981.

[2] N. Inaba, T. Saito and S. Mori, “Chaotic Phenomena in a Circuit with a Negative Resistance and an Ideal Switch of Diodes,” *IEICE Trans.*, vol. E-70, pp. 744–754, 1987.

[3] H. Sekiya, S. Moro, S. Mori, and I. Sasase, “Synchronization Phenomena on Four Simple Chaotic Oscillators Full-Coupled by Capacitors,” *IEICE Trans. Fundamentals*, vol. J82-A, No. 3, pp.375–385, 1999.

[4] M. Miyamura, Y. Nishio and A. Ushida, “Clustering in Globally Coupled System of Chaotic Circuits,” *IEEE Proc. ISCAS’02*, vol. 3, pp. 57–60, 2002.

[5] L. M. Pecora and T. L. Carrol, “Synchronization in Chaotic Systems,” *Physical Review Letters*, vol. 64, pp. 821–824, 1990.

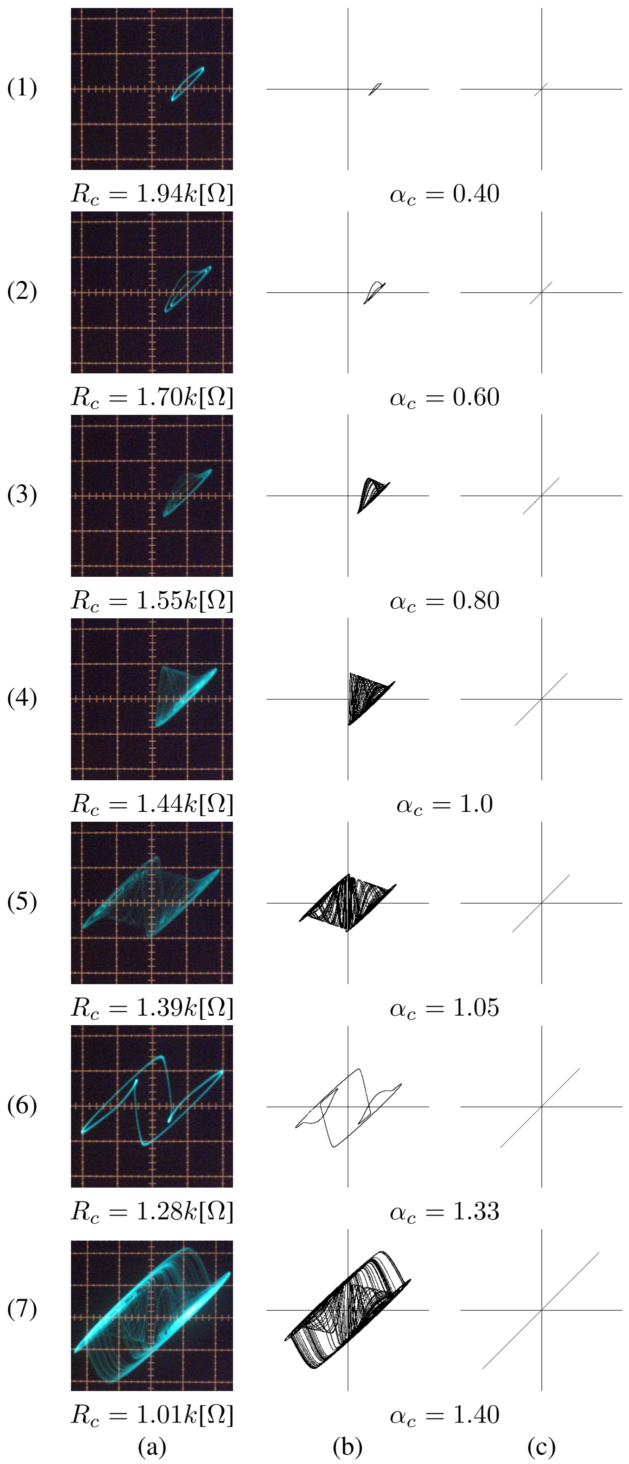

Figure 3: Circuit experimental results (left) and computer calculation results (center and right) ($N = 2$). $R_1 = R_2 =$[Ω], $R_3 =$[Ω], $C_1 = C_2 =$[μF], $C_c =$[μF], $\alpha_1 = 4$, $\alpha_2 = 9$, $\beta_2 = \beta_3 = 0.32$, $\gamma_1 = \gamma_2 = 1$, (a) Projection of attractors onto $v_3 - x_1$ plane. (b) Projection of attractors onto $x_3 - x_1$ plane. (c) Poincaré sections. $x_1 - x_2$ plane.

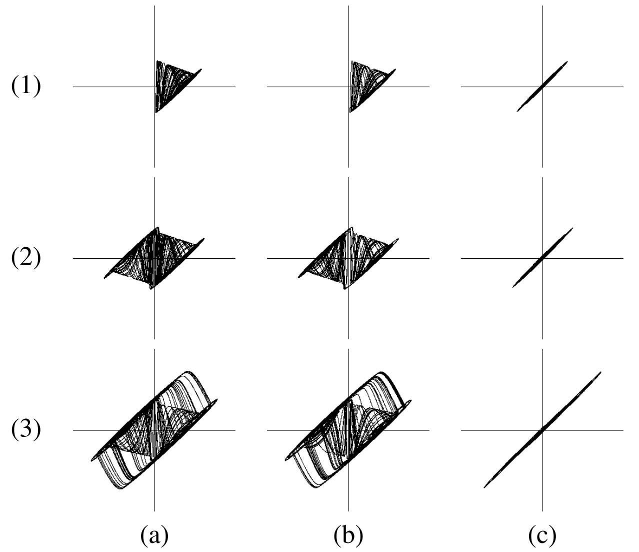

Figure 4: Different capacitances case. $C_1 = 1.0$ and $C_2 = 1.0$. (a) $x_3 - x_1$. (b) $x_3 - x_2$. (c) $x_1 - x_2$. (1) $\alpha_c = 1.0$. (2) $\alpha_c = 1.1$. (3) $\alpha_c = 1.5$.

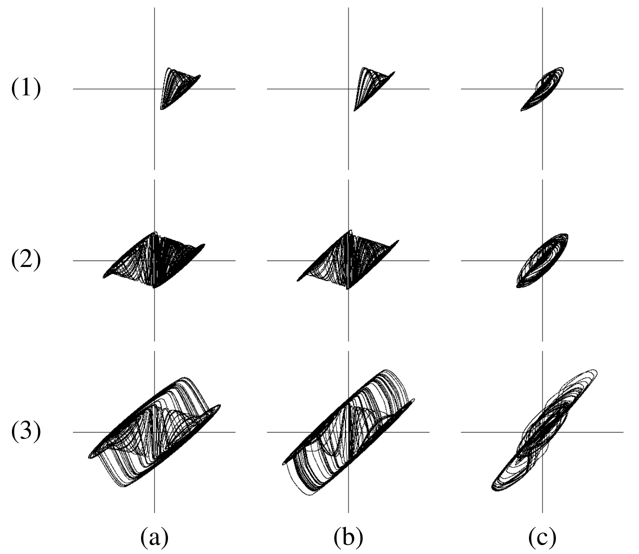

Figure 5: Different resistance case. $\alpha_1 = 4.0$, $\alpha_2 = 9.0$, $\beta_2 = \beta_3 = 0.32$ and $\gamma_1 = \gamma_2 = 1$. (1) $\alpha_c = 1.00$. (2) $\alpha_c = 1.05$. (3) $\alpha_c = 1.60$. (a) $x_3 - x_1$. (b) $x_3 - x_2$. (c) $x_1 - x_2$.

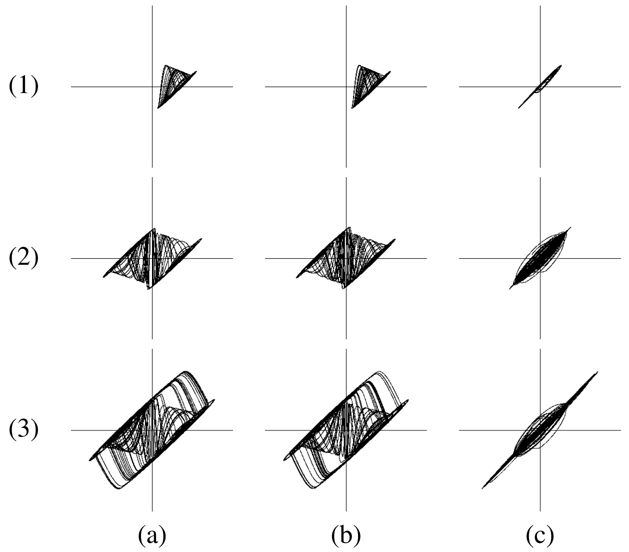

Figure 6: Different capacitances case. $C_1 = 1.1$ and $C_2 = 1$. (a) $x_3 - x_1$. (b) $x_3 - x_2$. (c) $x_1 - x_2$. (1) $\alpha_c = 0.9$. (2) $\alpha_c = 1.1$. (3) $\alpha_c = 1.5$.

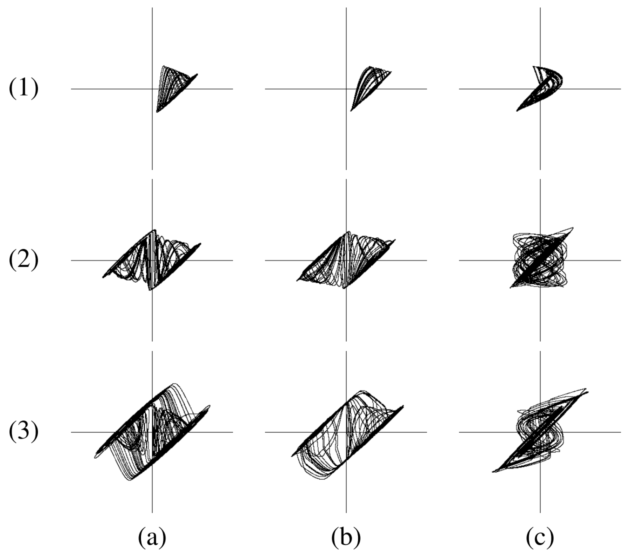

Figure 7: Different capacitances case. $C_1 = 0.33$ and $C_2 = 1.0$. (a) $x_3 - x_1$. (b) $x_3 - x_2$. (c) $x_1 - x_2$. (1) $\alpha_c = 1.0$. (2) $\alpha_c = 1.2$. (3) $\alpha_c = 1.6$.